CHAPTER-FOUR

MAGNETIZATION IN $Zn_xMg_{1-x}Fe_2O_4$ FERRITE SYSTEM DOPED WITH 0.1 MOL. Wt % ZrO_2

4.1 Introduction :

Hystersis studies on ferrites provide an useful information from the practical point of view. The data that governs the magnetic behaviour such as, permeability (μ), saturation magnetisation (Ms), coersive force (Hc), remmanance and the Mr/Ms ratio can be derived from the nature of hystersis loop exhibited by the material. The general range of coersive force varies from 0.1 Oe to 3000 Oe for ferrites. Ferrites are classified into hard and soft by the nature and coersive force. Ferrites with low values of Hc are called soft ferrites. They are used in high frequency inductance cores of transformers, motors and generators. The hard ferrites with large 'Hc' are used for permenent magnets, electric motors, loud speakers, telephones and T.V. receivers.

Neel[1] in 1949 has shown that coresive force Hc is related with the crystal anisotropy, saturation magnetisation, the internal stresses and the porosity. The squareness of hystersis loop determines their use in magnetic memory and switching devices. Magnetic properties of ferrites are influenced by physico-chemical and thermal hystory. Maxwell has suggested the experimental method for the measurement of magnetic properties of ferrites. For the sake of measurement of magentic parameter we have used the hystersis loop tracing method; for the system Zn_x Mg_{1-x} Fe_2O_4 doped with 0.01 mol. wt. % ziroconium oxide under investigation. A part of this chapter is also devoted to some theoretical aspects, in brief, to enable the interpretation of the data obtained.

4.2 Classification of magnetic materials and spin ordering :

Susceptibility, χ, is the unique property of magnetic materials, that establishes the relationship between the magnetisation M and an applied field H given by

$$\chi = \frac{M}{H} \quad \text{.....} \quad (4.1)$$

For diamagnetic material suceptibility X is less than zero, or negative and for paramagnetic materials it is positive. The temperature dependance of susceptibility in paramagnetic materials is given by

$$\chi = \frac{C}{T} \quad \text{.....} \quad (4.2)$$

Where C is the Curie constant the value of which from quantum statastic predicted by Maxwell is

$$C = \frac{\mu_{eff}\ Ms}{3\ k} \quad \text{.....} \quad (4.3)$$

where μ_{eff} is the effective value of magnetic moment. For paramagentic materials with strong L- s coupling with H, value of μ_{eff} is given by

$$\mu_{eff} = g \,/\, J(J+1)\ \mu_B \quad \text{.....} \quad (4.4)$$

Where the notations are having their usual meanings. The expression 4.2 is also called as Curie law.

The paramagnetic materials can be subdivided into ferromagnetic, ferrimagnetic and antiferromagnetic materials on the basis of their spin ordering. The possible spin ordering in these materials is as shown in fig. (4.1).

Ferro and ferrimagnetic materials show sponteneous magnetisation below Curie temperature and above it a normal paramagnetic behaviour. The antiferromagnetic material is a special class of ferromagnetic materials in which there is no spontaneous magentisation because of equal and opposite magnetic moments. The susceptibility variation with temperature in ferromagnetic and

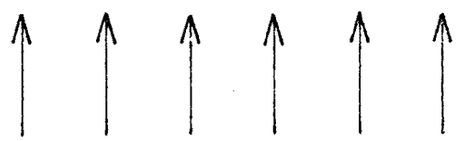

SIMPLE FERROMAGNETIC SPINS

SIMPLE ANTIFERROMAGNETIC SPINS

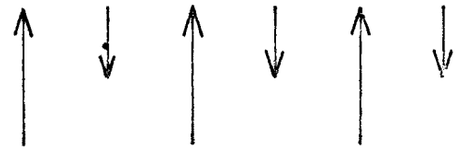

FERRIMAGNETIC SPINS

CANTED ANTIFERROMAGNETIC SPINS

Fig. 4·1 : THE POSSIBLE SPIN ARRANGEMENTS

ferrimagnetic shows deviation from Curie law and is given by a more general law called as Curie-Weiss law as

$$\chi = \frac{C}{T - T_C} \quad \text{.....} \quad (4.5)$$

Above expression is based on Weiss nature of molecular field in ferrimagnetic and ferromagnetic materials. In antiferromagnetic materials the relation is given by

$$\chi = \frac{C}{T + T_C} \quad \text{.....} \quad (4.6)$$

The positive sign in above expression is due to antiparallel coupling of magnetic spins. The 'T_C' in these materials represents critical temperature below which there is a sponteneous magnetisation. In antiferromagnetic material the disordering temperature is called as Neel temperature.

4.3 Origin of domains and energy considerations :

To explain the existance of sponteneous magnetisation in ferromagnetic materials Weiss in 1907 postulated the existance of molecular field. This molecular field tries to orient the atomic molecular magnets to give non-zero magnetisation in the absence of field. The variation of magnetisation with applied field can not occur gradually. This fact was suggested by Barkhausen[2] used to support the magnetisation by domain rotation. Landu and Lifshiftz showed that the domain structure is a natural consequence of exchange energy, anisotropy energy and magnetostatic energy. The origin of domains and Weiss nature of molecular fields remains unknown until Heisenbergs[3] (1928) theory of exchange interaction. With the theory of exchange interaction he was able to explain sponteneous magnetisation in ferromagnetic material having parallel spins.

Neel[4] in 1948 showed the existance of antiparallel spins and a negative exchange interaction. Further he extended his theory to account the spontaneous magnetisation in ferrimagentic material by assuming unequal antiparallel arrangement of spins. According to Neel the origin of domains in ferromagnetic solids can be understood from the thermodynamic principle; that in equilibrium energy of the system is minimum. Therefore we first consider the total energy of a ferromagnetic solid and then consider how it is minimised. The total energy comprises the sum of exchange energy, the anisotropy energy magnetostatic energy, magnetostriction energy and wall energy given by

$$E = Ex + Ek + Em + Ew + E\lambda \quad \ldots\ldots \qquad (4.7)$$

4.3(a) Exchange energy : Exchange interaction between the near neighbouring atoms leads to exchange energy. By neglecting anisotropy effects, the value of exchange energy is given by the relation

$$Eex = 2JS^2 \sum_{i>j} \cos \phi_{ij} \quad \ldots\ldots \qquad (4.8)$$

where S is the total spin moment per atom and ϕ_{ij} is the angle between the two spin moment vectors i and j. Exchange energy is lowered when spins are parallel. It thus favours an infinitely large domains in the speciman that is a single domain. It's value is approximately equal to 10^{-35} ergs per cm^3.

4.3(b) Magnetic energy : Magnetised speciman has a free poles at its ends, and thus produces an external field H. This field is due to magnetic energy. The magnitude of this energy is given by the relation

$$Em = \frac{1}{8\pi} \int H^2 \, dv \quad \ldots\ldots \qquad (4.9)$$

where the integration covers whole range of field H. This is a high value of energy being for a square crossection of the order of Ms^2 approximately

equal to 10^6 ergs per cm^3. Where Ms denotes the saturation magnetisation. This is lowered if the volume in which the external field exists is reduced and it is eliminated if the free poles at the ends of speciman are absent.

4.3(c) Anisotropy energy (Ek) : The excess of energy required to magnetise the speciman in a given direction over that required for the easy direction is called as the anisotropy energy. For the cubic material with α_i directional cosines, anisotropy energy will be

$$Ek = K_1(\alpha_1^2\alpha_2^2 + \alpha_2^2\alpha_3^2 + \alpha_3^2\alpha_1^2) + K_2(\alpha_1^2\alpha_2^2\alpha_3^2) \quad \ldots\ldots (4.10)$$

Where K_1 and K_2 are anisotropy constants, depending upon the nature of material and temperature. The constants are determined directly by measuring (5,6,7) the mechanical torque ona single crystal of the material as the direction of M. The value and sign of k determines the direction where Ek is minimum.

The physical origin of the anisotropy energy is however obscure. It can not have a direct relation with exchangeinteraction because it only concerns with the direction of spins and the crystal axis and not on the angle between the spin. When the magnetisation vector deviate from the preferred direction the anisotropy energy increases. For K_1 greater than zero the value of Ha is given by the relation

$$Ha = \frac{K_1}{2Ms} \quad \ldots\ldots \quad (4.11)$$

4.3(d) Magnetoelastic energy ($E\lambda$) : Change in dimension of a ferromagnetic material when magnetised give rise to magnetostriction energy. It arises due to interaction between magnetisation and strain developed due to magnetisation. It is given by

$$E\lambda = 3/2\ \lambda T \sin^2\theta \quad \ldots\ldots \quad (4.12)$$

Where T is the tension, θ the angle between magnetisation and strain and λ is the magnetostriction coefficient. Magnetostriction energy changes the anisotropy energy and also influence the size of the domain wall. It has effect in increasing the internal magnetic fields and also contribute to magnetic losses in ferrites.

4.3(e) Domain wall energy (Ew) : Bloch[8] in 1932 showed that the entire change in spin direction between the domains magnetised in different directions does not occur in one sudden jump across the single plane. Rather, the change of direction takes ina gradual way extending over many atomic planes. The reason for this gradual change is the minimisation of exchange energy. In this process of gradual change the atomic spins within the wall do not remain parallel to any easy direction and therefore lead to some anisotropy energy. According to the rotation of spins in the domain walls as 180°, 90° domain wall. The thickness of the domain wall is determined by the condition of minimum total energy given by

$$Ew = \frac{4}{(Ak)^{1/2}} \qquad \ldots\ldots \qquad (4.13)$$

where A is the exchange energy constant and K the anisotropy constant.

4.4 Wall Formation :

The optimum domain configuration lies in the principle of minimisation of above discussed sum of domain energy, from the saturation to zero value of magnetisation. We know that across a Bloch wall their will be no divergence of magnetisation when it changes from one direction to any other direction of magnetisation. Neel[9] pointed out that if a wall thickness is equal to the thickness of specimen then the interaction between free poles of strips formed

by intersections of the wall with the specimen surface becomes important. In case of thin films Neel walls becomes energeticaly fevoured. In Neel walls magnetisation rotates from one direction to near neighbouring one while remaining in the plane of the film. Middlehoek[10] extended Neel's work in which energy form different transitions is given as a function of angles between orientations of the neighbouring domains.

From the theory it is found that Bloch wall is formed in a specimens of thickness greater than 900 A° approximately. And below which cross tie walls are favoured. These theorotical considerations does not allow the Neel wall formation, however in specimen of thickness less than 200 A° Neel walls are observed. Besides these more complex walls with complex spin rotations found to exist in which alternate sections of Bloch and Neel type of transition regions forms continuty. By experiment it is evident that dimensions of grains and interaction between the adjecent grains that modifies the domain pattern. This is true for polycrystalline ferrites as well as for single crystals.

4.5 Domain wall and irreversibility :

Domain wall is the layer that separates the regions of different orientations. It is also sometimes called as Bloch[8] wall. The irreversibility in wall motion is attributed to the impediments such as non-magnetic inclusions, defects and dislocations. A model of wall motion proposed by Kersten[11] in 1943 in homogenious materials containing inclusions shows change in energy of the domain wall resulting in the variation of wall area. The irregular dispersion of wall impediments in the same domain may affect the magnitude and direction of magnetisation. Neel with this dispersed field theory calculated the critical field Hc required for irreversible domain wall moments and

coercivity. The effects of granular inclusions, lamellar precipittates, grains boundries and crystal faces was studied by Goodenough[12] in 1954 and have concluded that these are the most likely centres of the reverse domain formation.

4.6 Hystersis and coercivity :

Ferromagnetic material in its dimagnetised state consists of a large number of small magnetic regions called domains. The random orientations of these domains give zero net magnetisation. The orientations of the domains can be altered by application of magnetic fields to give non-zero magnetisation The magnetisation process takes place by two means, domain rotation and domain wall displacement that is by domain growth (See Fig. 4.2 (a))

The magnetisation is reversible at low applied fields and is temperature dependant. At high fields the magnetisation takes place due to domain wall rotation. This process of magnetisation is irreversible and is temperature independent. The irreversible domain wall motion is due to the fact that the boundry is forced across crystal imperfections, inclusions, grains and other physical barriers.

The entire cycle of magnetisation consists of reversible and irrreversible wall motion and roation of domain walls at high fields. The plot of change of magnetisation with applied external H is called hystersis loop as shown in Figure 4.2(b). In ferromagnetic materials the hystersis is due to irreversible wall motion at low applied fields. From the figure 4.2(b) it can be seen that, to bring the magnetisation M to be equal to zero the reverse field is necessary called Hc, the coercive force. The value of magnetisation at H=0 called the remannance Mr. The maximum value of magnetisation of high applied field is called saturation magnetisation Ms. The saturation induction Bs is 4π times the saturation magnetisation ms.

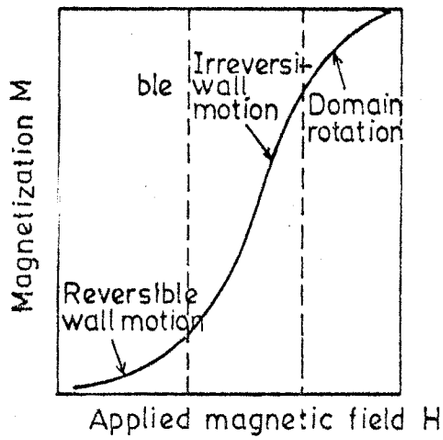

Fig.4·2a: A TYPICAL MAGNETIZATION CURVE

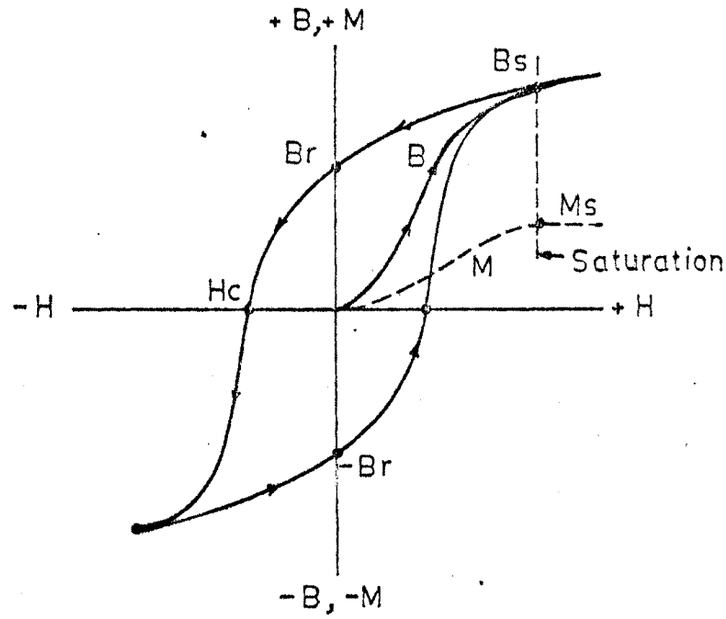

Fig.4·2 b: GENERAL FEATURES OF HYSTERESIS LOOP

Coercivity : The coercive force Hc depends on the grain size of the polycrystalline material. It is found that coercive force increases with decreasing particle size reaches to maximum and then tends to zero. The high coercive force is required for the permanent magnetic applications. Particle size is the main cause for coercive force and hence in all ferrites systems the efforts are being made to control the grain size by using hot pressing techniques. The variation of coercivity with particle size is as shown in figure 4.3. The figure distinguish the following regions :

4.6(a) Multidomain (M- D) : Magnetisation of the specimen containing M-D particles changes by domain wall motion. The variation of Hc in most of the cases can be approximated by the expression

$$Hc = a + b/D \quad \ldots\ldots \quad (4.14)$$

Where a and b are constants and D is the particle diameter.

4.6(b) Single Domain (S - D) : When the particle size reduces below critical diameter Ds, reaches to single domain particle size, then Hc will be maximum. Decrease of coercivity below critical diameter is attributed to thermal effects and is presented by the relation

$$Hc = g - h/D^{3/2} \quad \ldots\ldots \quad (4.15)$$

Where g and h are constant.

When particle size (diameter) is below Dp, the coercive force Hc is zero and it is attributed thermal effects. Now in this stage the thermal effects are strong enough to demagnetise the already saturated assembly of particles. The particle size in this respect is called superparamagnetic (Sp) Coercivity is also influenced by shape anisotropy, when powder compaction is used. Due to shape anisotropy the coercivity of aligned elongated particles

M-D = Multi-domain
S-D = Single domain
SP = Superparamagnetic

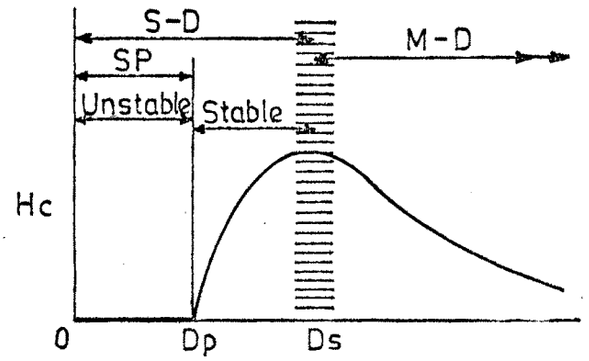

Particle diameter D

Fig. 4·3 : VARIATION OF COERCIVITY WITH PARTICAL DIAMETER.

reversing by coherent rotation proposed by Stoner and Wohlforth[13] show distinct discrepancies with the theoretical, showing the existance of nonparallel spins. The most important modes of these are magnetisation Fanning and Curling[14]. A fanning reversal is characterised by a rectangular hystersis loop and the coercivity in this mode is given by

$$Hc = \pi Ms/2 \quad \ldots\ldots \quad (4.16)$$

Frei Shtrikinan and Treves[15] investigation on coercivity in curling mode shows size dependance. If crystal anisotropy K is large then large particle size also shows substantial coercivity. The Hc in this case is given by

$$Hc = 2k/Ms \quad \ldots\ldots \quad (4.17)$$

4.7 Losses in Magnetic Materials :

Magnetic materials absorbs certain energy in an alternating magnetic field and dissipates it in the form of heat. If the alternating field is

$$H = Ho \exp (iwt) \quad \ldots\ldots \quad (4.18)$$

Then the induction B can be written as

$$B = Bo \exp\ i(wt + \delta) \quad \ldots\ldots \quad (4.19)$$

So that $$\mu = \frac{B}{H} = \frac{Bo}{Ho} (\cos \delta + i \sin \delta)$$

$$\mu = \mu' + \mu'' \quad \ldots\ldots \quad (4.20)$$

Where μ' is the component of flux in phase and u" is the component of flux out of phase by 90° with applied field. The loss in energy is found to be proportional to μ''.

The power factor or loss factor is given by

$$\tan \delta = u''/\mu' \quad \ldots\ldots \quad (4.21)$$

The quality factor Q is given by

$$Q = \mu'/\mu'' = 1 / \tan\delta \quad \ldots\ldots \quad (4.22)$$

The variation of μ' and μ'' with frequency can provide an useful information from the application poit of view.

The losses in the magnetic material are due to following important mechanism[16] such as,

1) Hystersis 2) eddy current 3) Spin resonance 4) relaxation and 5) wall resonance. In ferrites at low fields the losses are due to hystersis and eddy current are of loss important in comparision with the other sources of losses.

4.7(a) Hystersis loss : To change the magnetisation from M to M +dM in an applied field H, the energy required is given by

$$dE = H.dM \quad \ldots\ldots \quad (4.23)$$

Then the energy absorbed for a complete cycle is given by

$$W = \oint H.dM \quad \ldots\ldots \quad (4.23)$$

It is nothing but the area under the hystersis loop. For low hystersis loss area under the curve must be small. Low coercivity and high permeability are the requirement for small loop area.

4.7(b) Eddy current loss : When an alternating magnetic field is employed to magnetic core materials, an electric current is induced in the material that causes the power loss. The power loss per second is found to be proportional to f^2/ρ, where f is a frequency of applied field and 'ρ' be the electrical resistivity of the core material. The constant of propertionality in this respect depends on the shape of core.

4.7(c) Spin-resonance loss : The precessional frequency w of an electron spin vector in the presence of internal anisotropy field Hk is given by

$$w = \gamma Hk' \quad \ldots\ldots \quad (4.24)$$

Where 'γ' is the gyromagnetic ratio. If now an external field Hi (r.f. field) is applied in a direction normal to Hk' then the maximum energy is absorbed, when the frequency of precession becomes equal to the frequency of r.f. magnetic field, a condition for the resonance is satisifed. For a material with negative anisotropy, the rotational process is important and the resoanant frequency in this case is found to be inversly proportional to (μ - 1). Hence higher the permeability lower is the resonance frequency and viceversa.

4.7(d) Relaxation loss : The losses that occurs at frequencies much lower than resonant frequencies have significant contribution to the magnetic losses. These losses are attributed to several relaxation losses in ferrites, due to electron exchange between Fe^{2+} and Fe^{3+} ions for minimum energy, that results in change of magnetisation direction. The relaxation loss is found to be frequency dependent and is maximum at applied frequency equal to relaxation frequency for electron jump for a given material at a given temperature.

4.7(e) Wall resonance loss : The domain wall resonance losses are found to occur in some ferrites at low frequency. If the domain wall is disturbed from its equilibrium position develop restoring forces in it; that tries to bring it back to original position. Hence domain wall behaves as a stretched elastic membrane having some natural frequency of oscillation. When the frequency of applied field becomes equal to the natural frequency, the wall resonance takes place resulting maximum absorption of energy.

4.8 Experimental set up and Measurement Technique :

For the hystersis measurement we have used high field loop tracer supplied by Arun electronics private limited, Bombay. It consists of an alternating current electromagnet working on 50Hz; with the aid of which an alternating field of maximum 3500 Oe is produced in an air gap of 9 mm as shown in plate (4.4). The signal from the balancing coil is integrated and fed to vertical deflecting plates of cathode ray oscilloscope with suitable amplification. The balancing coil that detects the magnetisation of sample collects the signal proportional to magnetic moment of specimen. At the same time a signal proportional to magnetic field has been fed to horizontal deflecting plates of cathode ray oscilloscope. The vertical deflection is calibrated in emu and the horizontal in terms of Oresteds per division. The calibration was made with the standard nickel strip having magnetisation of 53.34 emu per division. To obtain the hystersis loop on C.R.O. screen the following method is used.

At first high voltage cable was connected from the control unit to the 'C' core unit. The balancing coil was slowly introduced into the air gap after connecting it to twelve pin connector associated with the 'C' core unit. The outputs (V,H) are connected to input (V,H) of the control unit. The current range was kept at one Ampere position, with current control at minimum position. The vertical output of the control unit was connected to the vertical cnannel of the oscilloscope. The horizontal output was connected to the external input of the oscilloscope. The vertical gain control was kept at low positive, with the help of current control knob. The current was increased upto 220 mA so as to obtain an eclipse on screen. By adjusting vertical phase

control the ellipse was converted into the straight line. Now by adjusting potentiometer by coarse knob phase difference was confirmed which shows only rotation of straight line and was made zero by adjusting phase potentiometer.

With this setting, the balancing coil was slowly taken out of 'C' core gap and the pallet sample was slowly inserted into an air gap. The current was slowly increased to obtain saturation magnetisation and a hystersis loop was displayed on screen. With the help of camera for each samples of $Zn_xMg_{1-x}Fe_2O_4$ (where x = 0, 0.2, 0.4, 0.6, 0.8, 1.0) ferrite system doped with 0.01 mol. wt.% ZrO_2, photographs are taken, under the same are represented in the plate 4.5.

With the help of calibrated plate (1 MA = 0.1 volt) from corresponding effective lengths of hystersis loop and excited fields in the 'C' core, the saturation magnetisation (Ms) in emu per cm^3 were obtained at room temperature. From the measurements of Ms values, n_B the saturation magnetic moment can be calculated by the expression

$$n_B = \frac{Ms\ W}{5585 \times ds} \quad \ldots\ldots \quad (4.26)$$

where w is the molecular weigyht and d be the density of material sample. We have also calculated the value of α_{yk} angles. The data obtained is represented in table 4.1.

4.9 Results and Discussion :

In figure 4.6 compositional variation of saturation magnetisation (Ms) has been shown for the ferrites $Zn_xMg_{1-x}Fe_2O_4$ system doped with 0.01 mol. wt. % ZrO_2. From figure 4.6 it is seen that the content of zinc is increased

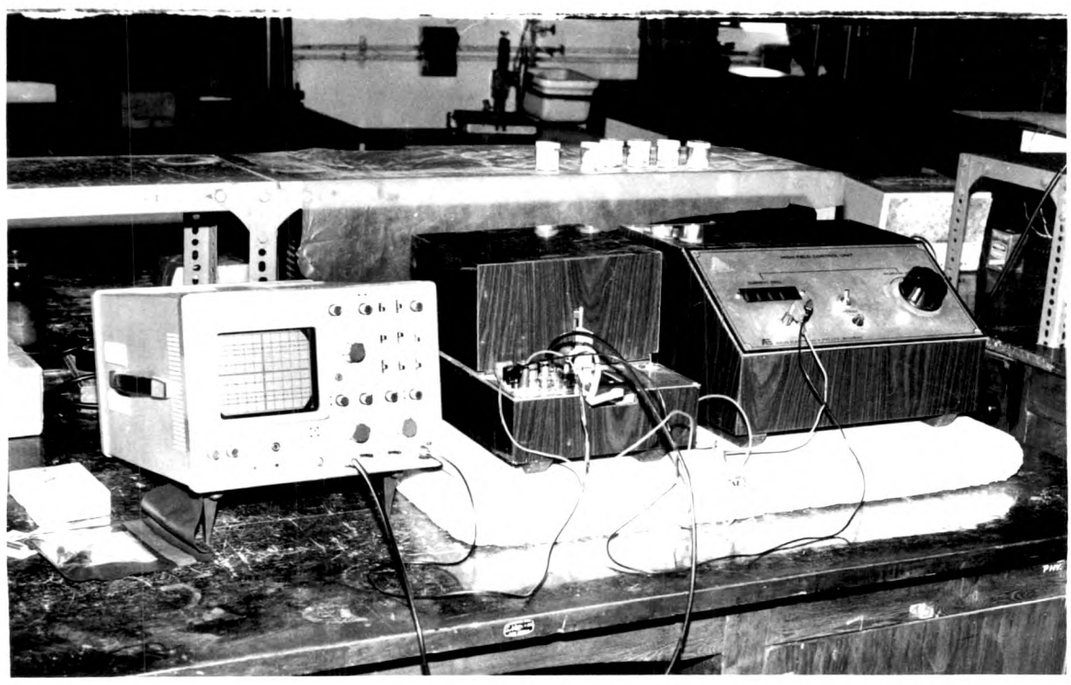

FIG-(PLATE) 44: EXPERIMENTAL SETUP FOR HYSTERSIS MEASUREMENTS

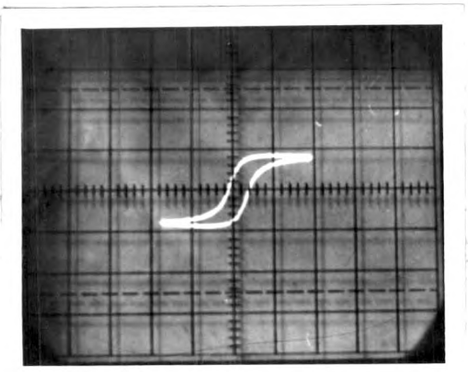

L0

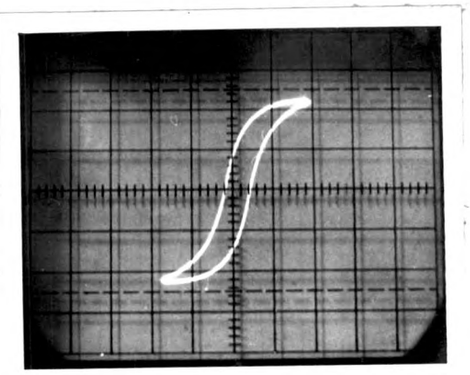

L2

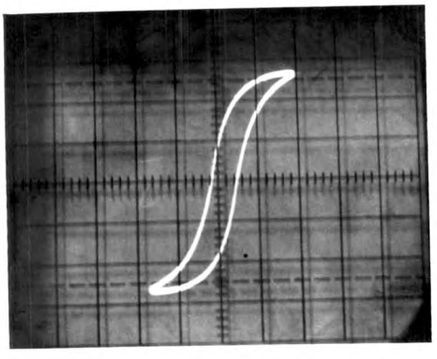

L4

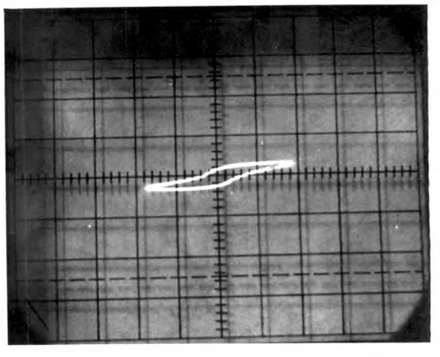

L6

FIG- (PLATE) 4.5 : HYSTERSIS LOOP ON C.R.O.

133

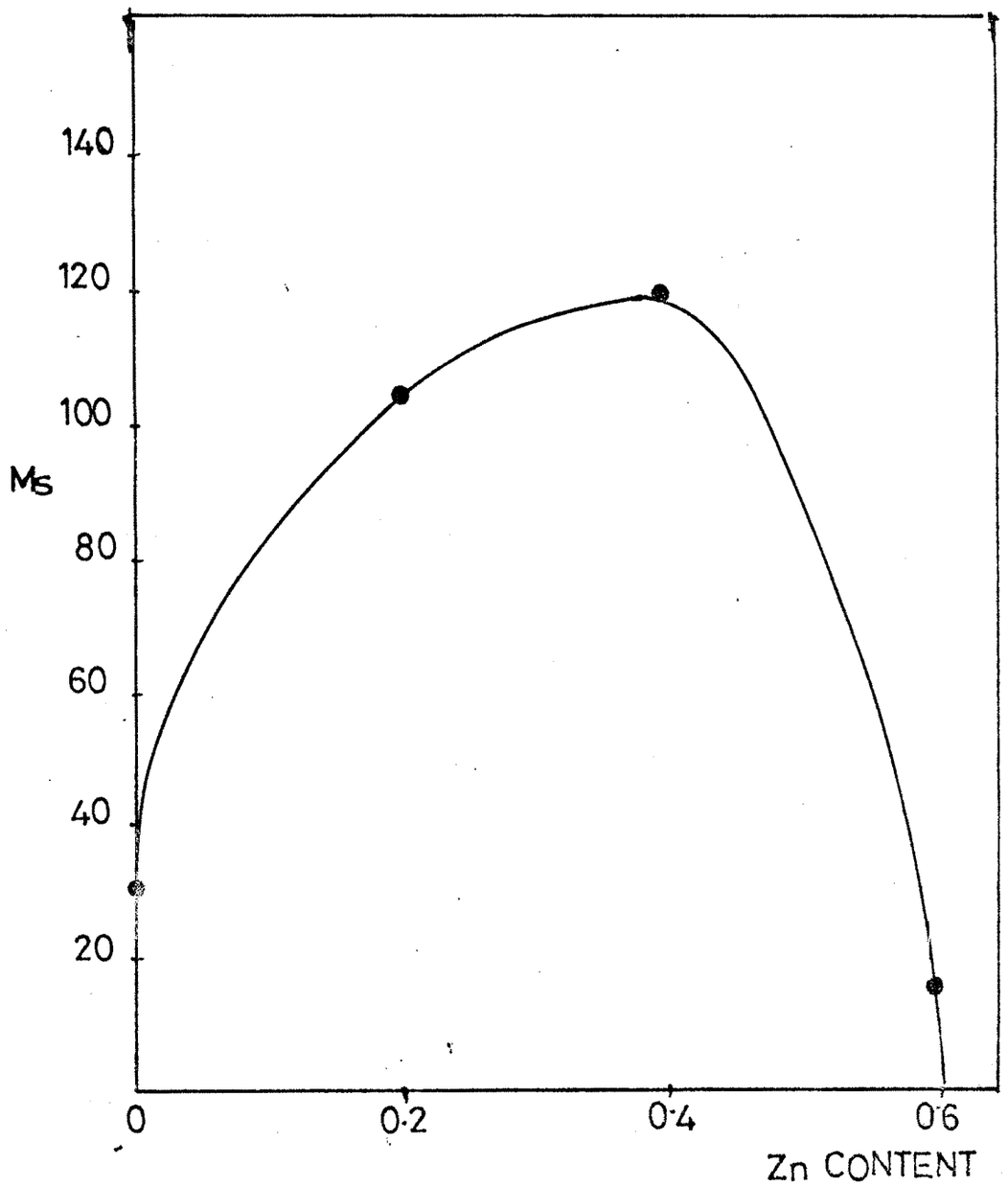

FIG-4·6 Ms Vs Zn CONTENT

Table 4.1

Magnetic data obtained for slow cooled $Zn_xMg_{1-x}Fe_2O_4$ ferrite system doped with 0.01 mol. wt.% ZrO_2

Composition 0.01 mol. wt. % ZrO_2	Sample Notation	6s emu/gm	Ms emu/cm^3	α_{yk} for doped system	α_{yk} for undoped (21)	Tc doped	Tc undoped (21)
$MgFe_2O_4$	L_0	13.8554	29.3772	0.3389	0	0	440.2	482
$Zn_{0.2}Mg_{.8}Fe_2O_4$	L_2	40.7659	105.4210	1.1291	34°18'	0	328.6	375
$Zn_{0.4}Mg_{.6}Fe_2O_4$	L_4	44.063	119.7485	1.2753	48°08'	30°75'	228.6	282
$Zn_{0.6}Mg_{.4}Fe_2O_4$	L_6	4.9	13.63	0.1474	71°01'	66°08'	127.0	145
$Zn_{0.8}Mg_{0.2}Fe_2O_4$	L_8	-	-	-	90°	90°	-	-
$ZnFe_2O_4$	L_{10}	-	-	-	90°	90°	-	-

the value of Ms also show increasing trend upto 40% zinc content, beyond which a decreasing trend is exhibited. This result is in good agreement with zinc substituted mixed ferrites $Zn_xMg_{1-x}Fe_2O_4$, where M represents divalent cation (16,17). However it can be seen that the effect of doping ziroconium in Zn-Mg mixed ferrites is that the Ms values are generally declined. The decrease in Ms values beyond certain composition is attributed by N.S. Satyamurthy[18] to the existance of canted spin beyond this composition in the ferrites. Similar results has been reported by V.R. Kulkarni[19] for Cu - Cd system. They have calculated α_{YK} angles.

Srivastava[18] et. al. have calculated Y.K. angles for $Zn_xFe_{3-x}O_4$, R.G. Kulkarni[20] et. al. have carried out studies on magnetic ordering in Cu-Zn ferrites. They have calculated theoretical values of YK angles using the formulla

$$\cos \alpha_{yk} = \frac{5(1-x)^2 + 25(1-x)^2}{(1-x)^2 + 25(1+x)^2 + 10(1-x)^2}$$

They have used the values of exchange constant as follows :

$J_{AA} = -5.25$, $J_{BB} = -14.8$, $J_{AB} = -10$

$J_{AA} = 389$, $J_{BB} = -4.53$

Comparing the theoritical values of YK angles they have came to conclusion that canted spins are favoured on B sublattice, in the case of Cu-Zn ferrites. The following formula can also be sued for the calculation of YK angles.

$$\eta_B = (6+x) \cos\alpha_{yk} - 5(1-x)$$

where η_B is expressed in the units of Bohr magneton and x represents the content of zinc. The experimental values of magnetic moment were obtained by using the formula.

$$\eta\beta = \frac{\text{mol. wt. x Ms}}{5585 \times ds}$$

where ds is density of the samples and Ms saturation magnetisation in emu per cm^3. We have calculated values of Ms by using the formula

$$Ms = (1-p)\,\sigma s\, ds$$

where p is the porosity, and σs the saturation magnetisation in emu per gram.

The data of Ms, σs, αyk and experimental Tc values are represented in table 4.1, for $Zn_xMg_{1-x}Fe_2O_4$ ferrite system doped with 0.01 mol wt. % ZrO_2. Figure 4.7 show the vairation of $\eta\beta$ values in Bohr magneton with zinc content. It can be seen from figure 4.7, that values increases as Zn content increases, became maximum at about 40% of zinc, and beyond 40% it decreases. The results obtained in this case are in good agreement with Kulkarni[19] and Joshi[17] et. al. In sample Lo, no αYK angles are observed. This provides a sort of varification as $MgFe_2O_4$ strictly obeys the two sublattice model.

For the ferrites $Zn_xMg_{1-x}Fe_2O_4$ doped with 0.01 mol. wt.% ZrO_2 for the samples of (x = 0.2, 0.4, 0.6) the Neel's two sublattice model can be used to explain compositional variation of Ms, which is evidensed by the non zero YK angles. (See table 4.1). Thus the change in magnetisation on Zinc substitution occurs due to the presence of αYk angles in the spin system on B sites. For the table it can be seen that αyk angles are affected by ZrO_2 doping. For $Zn_{0.2}Mg_{0.8}Fe_2O_4$ no αyk angles are observed by Deshpande[21]. However on zirconium doping it is found to be positive and is of the order of 34°18'. Further, it can be seen from table 4.1, that they are more in all cases with respect to their undoped versions.

The observed increase in the αyk angles with zinc content in our case indicate that the increasing trend favours triangular spin arrangements on B

137

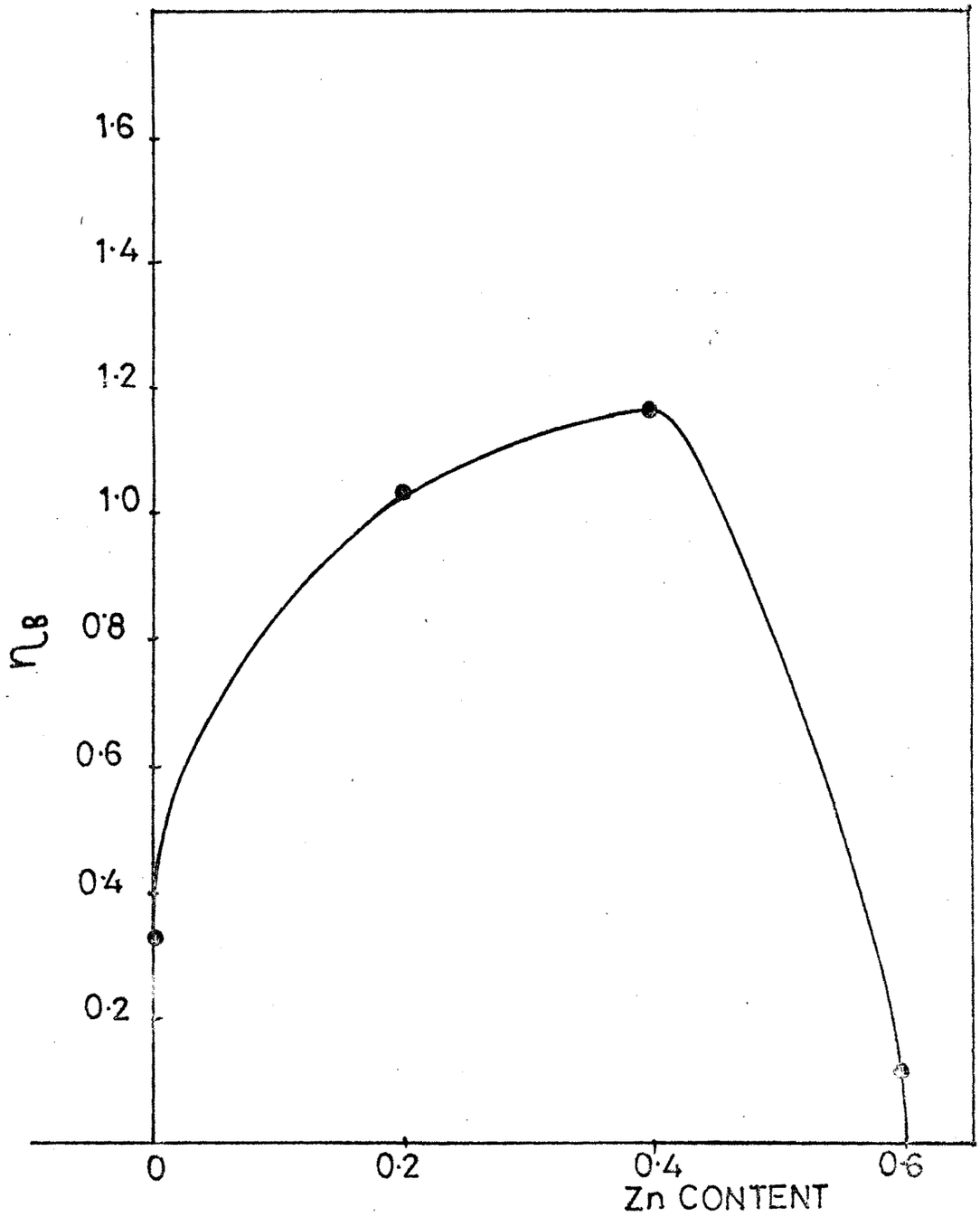

FIG-47 : η_B ※ Zn CONTENT

sites, leading to reduction in A-B interaction. B-B interactions are antiferromagnetic even in a mixed magnetic zinc ferrite. The effect of B-B interaction is usually masked by strong A-B interaction which causes the spin on B sites to be aligned parallel to each other. Therefore it can be concluded that $Zn_xMg_{1-x}Fe_2O_4$ ferrite system doped with 0.01 mol.wt.% ZrO_2 that lead to increased canted type of arrangements on B sites, weakening the A-B ntera-ction as suggested by Yafet[22] and Kittle.

The samples $Zn_{0.8}Mg_{0.2}Fe_2O_4$ ferrite doped with 0.01 mol wt.% ZrO_2 and $ZnFe_2O_4$ doped with 0.01 mol. wt.% ZrO_2 do not show any magnetisation. This is obvious because their Curie temperatures are below room temperature. This is in good confirmity with out results on conductivity in chapter III. For the above samples values are zero and YK angles equal to 90° The variation of Tc with Zn content is shown in figure 4.8. The lowering of Tc values can be co-related with observed values of α_{yk}. An increase in α_{yk} can be characterised by a decrease in A-B interaction leading to lowering of Tc.

The magnetic data obtained on $Zn_xMg_{1-x}Fe_2O_4$ ferrite system (undoped) do not show yk values for x=0 and x=0.2 [21]. From the table 4.1 it can be seen that Tc values in our doped system are lower than that of Deshpande[21] on the same system (undoped). This observed reduction in Tc values may be reflected in the increase of α_{yk} angles and hence the weakening of A-B interaction. This is in good agreement with the study of substitution of ion of a lower magnetic moment like Cu in Ni-Zn ferrite by Joshi[17] et. al. The study on 0.7 mol wt.% TiO_2 doped barium hexaferrite by D.Hennieke[23] et.al. have also observed reduction in Tc values, and have concluded that all additives occuping iron sublattices cause decrease in Curie temperature, our results are therefore in good agreement.

139

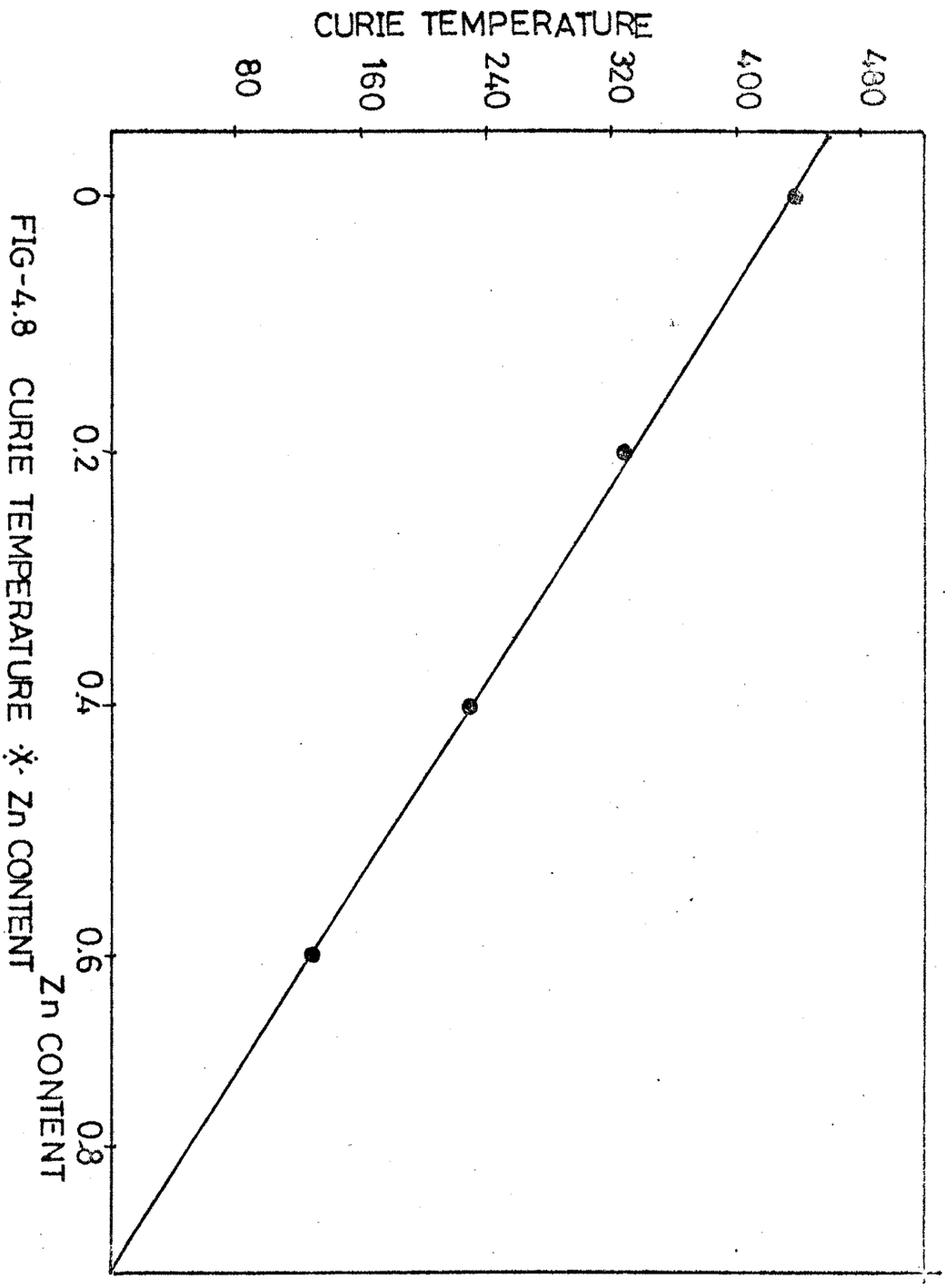

FIG-4.8 CURIE TEMPERATURE Vs Zn CONTENT

REFERENCES

1) Alper A.M. " High temperature Oxides", Academic Press, N.Y. 1971.

2) Barkhausen H., Phys. Zeits, 20, 401(1919).

3) Heisenberg W. Zent Fur Phys., 49, 619(1928).

4) Neel L., Ann. Physique. 3, 137(1948).

5) Bozorth R.M. " Ferromagnetism " Van Nastrand, New York (1951).

6) Chikazumi S, " Physics of Magnetism " Wiley and Sons, New York (1964).

7) Smit J. and Wijn H., H.P.J., Ferrites CEntrex, Eindhoven (1961).

8) Bloch F., Zeit Fur Physics, 74, 295 (1932)

9) Neel L., Compat. Rend. Acad. Sci. Paris, 241,533(1955).

10) Middlehoek S., J. Appl.Phys. 34, 1054(1963).

11) Kersten M., " Grundlagen Ciner Theorieder Ferromagnetischen Hysterese under Kuerzitivkraft ", Hirzel Leipzig (1943).

12) Goodenough J.B., Phys. Rev. 95 No.4, 917-932 (1954).

13) Stoner E.C. and Wohlfarth E.P., Nature, 160, 650(1947).

14) Frei E.H., Shtrikman S. and Treves D., Phys. Rev., 106, 446(1957).

15) Rao C.N.R. " Solid state chemistry ", Marul Dekker Inc. N.Y. 380 (1974).

16) Sinha A.P.D. and Menon P.G. " Solid state chemistry ", Ed. by C.N. R.Rao Marcel Dekker. INC. New York P. 387(1974).

17) G.K.Joshi, A.Y.Khot and S.R. Sawant, Solid State communications; 65 No.12, 1593-1595(1988).

18) N.S. Satyamurthy, M.G. Netera S.I. Youseef, R.J. Begum and C.M. Srivastava, Phys. Rev, 181 (2), 969(1969).

19) V.R. Kulkarni, Ph.D. Thesis, Shivaji University (1986).

20) R.G. Kulkarni and V.U. Patil, J. mater. sci., 17, 843(1982).

21) S.A. Deshpande M. Phil. Thesis, Shivaji University, Chapter IV (1987).

22) Y. Yafet and C. Kittel, Antiferromagnetic arrangements in ferrites 290(1952).

23) D. Hennicke, H.W. Hennike Powder metall. Inst. Germany 17, (5), 241-242(1985).